Microfabrication by two-photon lithography, and characterization, of SiO2/TiO2 based hybrid and ceramic microstructures

Anne Desponds, A. Banyasz, Gilles Montagnac, Chantal Andraud, Patrice Baldeck, Stephane Parola

Microfabrication by two-photon lithography, and characterization, of SiO_2/TiO_2 based hybrid and ceramic microstructures

Anne Desponds[1], Akos Banyasz[1], Gilles Montagnac[2], Chantal Andraud[1], Patrice Baldeck[1], Stephane Parola[1]

[1]*Université de Lyon, Laboratoire de Chimie, CNRS UMR 5182, Ecole Normale Supérieure de Lyon, Université de Lyon 1, 46 allée d'Italie, 69364, Lyon, France.*

E-mail: stephane.parola@ens-lyon.fr ; anne.desponds@ens-lyon.fr

[2]*Laboratoire de Géologie, CNRS UMR 5276, Ecole Normale Supérieure de Lyon, Université de Lyon 1, 46 allée d'Italie, 69364, Lyon, France.*

Abstract

High resolution fabrication using two-photon lithography is extensively studied for a large range of materials, from polymer to inorganics. Hybrid materials including a sol-gel step have been developed since two decades to increase mechanical or optical properties in particular on silicon based materials. Among the metal oxide, few studies have been dedicated to titanium and, because of the high reactivity of titanium precursors, obtaining a resin with a high part of titanium is challenging. Indeed, resins for two-photon lithography have to be stable for the processing time and titanium precursors are more difficult to operate due to their higher reactivity and often require drastic working conditions in order to control the chemical processes. Here, we propose a method, working at ambient conditions, to print submicronic structures of organic-inorganic hybrids with a large proportion of titanium and ceramics using high resolution two-photon process. The material obtained and its evolution during the pyrolysis at 600°C and 1000°C are characterized. We show that TiO_2/SiO_2 based micro-ceramics can be obtained after the pyrolysis of the microstructures. The respective roles of the two chemical reactions involved in this lithography process, sol-gel condensation and radical photopolymerization, are highlighted.

Figure abstract:

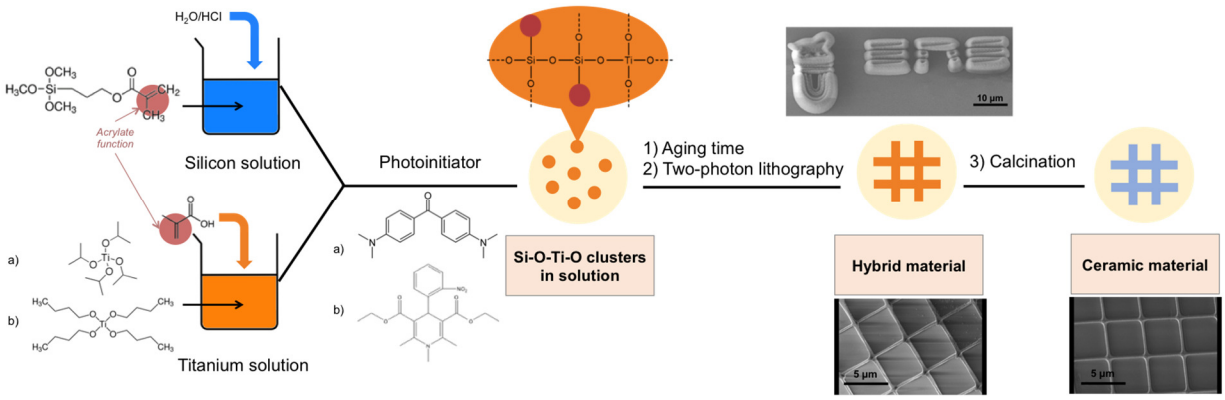

Highlights :

- 3D printing using two-photon absorption processes for the fabrication of high resolution at the submicronic scale of ceramic components
- Printing TiO_2 based ceramics of various compositions, controlling the resolution, structures and shape after annealing, is an important challenge and open perspective to large range of applications
- Two chemical reactions concomitantly involved during the process are critical, sol-gel condensation and radical photopolymerization.
- Sol-gel approaches towards high resolution 3D printed ceramics is an extremely promising method.

Keywords

Microfabrication; Ceramics; Sol-gel; Hybrids; Two-photon polymerization

1 Introduction

The patterning of sub-micrometric structures with high three-dimensional (3D) spatial resolution is in continual development to meet and improve the requirements of applications in various domains (automotive, aerospace, defense, healthcare, consumer, industrial automation, robotics, telecommunications). Most of the processes used to obtain the microdevices are composed of several steps including chemical and/or physical treatments [1], and the utilization of molds or masks, especially with inorganic materials [2, 3]. The multiphotonic lithography technic, also called "direct writing lithography", may replace these mixed processes which are heavy and complicated, through a fabrication by a 3D printing process involving reactions of radical photopolymerization. The two-photon lithography, based on a two-photon absorption process, has attracted a high level of interest due to its high spatial resolution, making possible the production of microdevices and microstructured surface. This technique was explored in the 90's and the 2000's [4–7]. Many materials are compatible with the two-photon lithography such as photopolymers [8], inorganic-organic material composed of silica precursors built up in organic network (ORMOCERS) [9], and its derivatives including titanium [10], zirconium [11, 12], or metal hybrids [13]. Full inorganic condensation sol-gel process has also been developed but remains hitherto limited to silica based materials [14, 15]. To obtain full inorganic materials, the fabrication in a polymeric matrix including inorganics followed by a debinding of the organic matter is a route that has been explored for SiCN microstructures [16], SiO_2/ZrO_2 [17] or SiOC [18].

The incorporation of TiO_2 in such micromaterials has been widely studied as this metal oxide presents excellent optical properties (high refractive index) while keeping electronic properties [19, 20]. Similar to the ORMOCER, inorganic-organic resins including Titania precursors have been studied for photonics [10, 21] pressure sensors [22] and biological [23, 24] applications. However, contrary to the silica precursors, the titanium is much more sensitive to the environment because of (i) its stronger electrophile character and (ii) its coordination number which is superior to its valence, making nucleophilic addition reactions possible when coordination of the metal is not complete [25]. Consequently, this metal center is very sensitive to reaction with ambient H_2O. To handle the titanium precursor and permit two-photon lithography resin, these compounds are stabilized by methacrylic acid to form less reactive clusters. These

reactions between alkoxides and ligands have been particularly studied [26]. It has been highlighted that the clusters formation are due to partial hydrolysis, thus making possible the incorporation of such compounds as building blocks for hybrid inorganic-organic matrix [27]. However, even under cluster form, the system remains very reactive. The addition of a silicon precursor makes it possible to reach a manageable composition but resins including a molar ratio Ti/Si superior to 1 are not achievable in these conditions, and the microstructures presented eventually a chipped surface aspect [10]. More recently, it has however being demonstrated that, under an argon environment without oxygen, the proportion of titanium precursor could be increased [22].

We propose here a simple route, in easily controllable conditions, to obtain ceramic microstructures with high titanium dioxide content from sol-gel based resins. The principle is to create mixed composite oligomers during the patterning of the microstructures, either by pre-hydrolysis and aging condensation of the alkoxide precursor, followed by two-photon polymerization, or by simultaneous two-photon controlled inorganic condensation and two-photon organic photopolymerization. We have noted that the type of titanium precursor has an influence on the stability of the resin. In particular, the replacement of the traditionally used titanium isopropoxide by the titanium butoxide allows us to increase the molar ratio Ti/Si up to 2.3 in the resin in our experimental conditions. Infrared spectroscopy allows characterization of the two chemical reactions involved during the transition from resin to micromaterial. In a one hand, the sol-gel condensation occurs, creating pre-form network and depending on the aging time, this reaction is more or less advanced. In another hand, the radical photopolymerization permits to connect the pre-form sol-gel network, and thus to form the micromaterial.

The fabricated microstructures of composite inorganic-organic hybrid can then be calcined to remove the organic and thus lead to inorganic microstructures with increased optical and mechanical properties. Such process towards Titania based ceramics remains barely studied. Here is reported the two-photon fabrication of TiO_2 based micro-ceramics from such hybrids.

2 Experimental

2.1 Chemicals

3-(Trimethoxysilyl)propyl methacrylate 98% (MAPTMS), 4.4-Bis(dimethylamino)benzophenone 98% (Michler's ketone) are purchased from Sigma-Aldrich. Titanium isopropoxide $Ti(O^iPr)_4$ (TiP) and titanium butoxide $Ti(OBu)_4$ (TiB) are purchased from Acros. Methacrylic acid (MAA) stabilized with 250 ppm MEHQ is bought from Alfa. The photobase "N-methylnifedipine ethyl ester derivative" is synthetized in our lab and the synthesis method is available elsewhere [15]. Concentrated hydrochloric acid 37% (HCl), and acetone 99% are purchased from VWR. The water (H_2O) used for synthesis is demineralized (18.2 MΩ.cm). The Michler's ketone is recrystallized in toluene: 8.1g of the product is recrystallized in 82.3g of toluene. The other chemicals are used without prior treatment. The chemical structures of the reactant used for the resin are presented in Fig. 1.

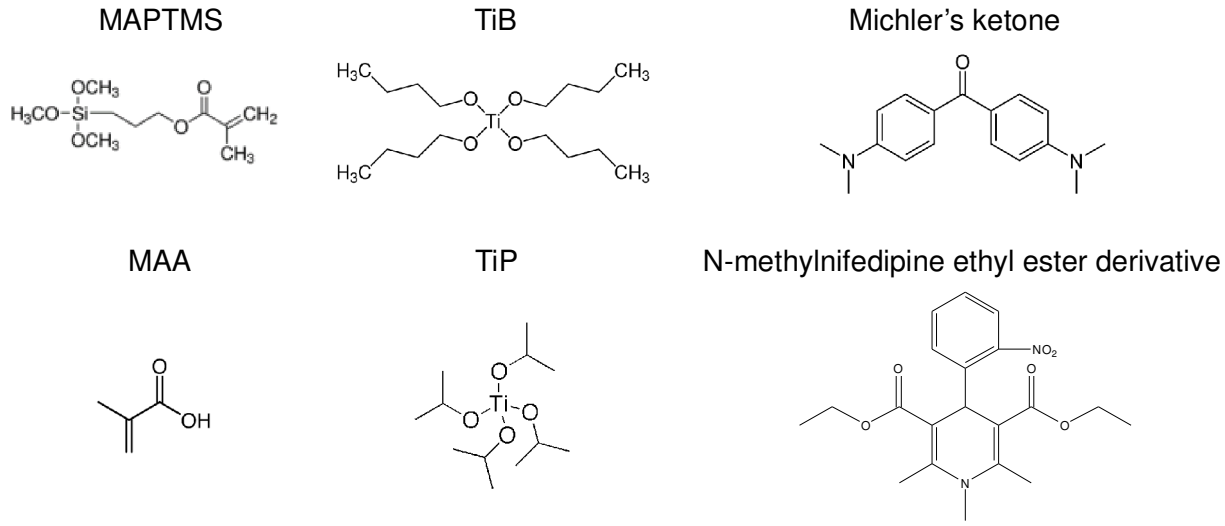

Fig. 1 Reactants used in the different hybrid resins

2.2 Photopolymerizable resins: MAPTMS/TiP/MAA

In an amber vial, the silicon precursor solution is prepared: a solution of MAPTMS at 80 wt% in acetone is prepared, and a solution of diluted HCl (0.1M) is added to hydrolyze the silane. In order to evaluate the influence of the hydrolysis conditions, four molar ratios of H_2O/MAPTMS (0.25, 0.5, 1 and 3) are considered (Table 1). The reaction medium is stirred for one hour.

Simultaneously, in another amber vial, the titanium precursor solution is prepared: a solution of $Ti(OiPr)_4$ (TiP) at 70 wt% in acetone is prepared and the MAA is added slowly under stirring, with a molar ratio equal to 1 (Table 1). The reaction is stirred for one hour.

Finally, the resin is prepared in a third amber vial. The silicon solution is added to the photoinitiator, Michler's ketone, (0.15 mmol). The titanium precursor solution is then dropped under stirring. The molar proportion of the TiP solution added to the MAPTMS solution is tuned between samples according to the following molar ratios Ti/Si: 0.4, 0.7, 1, 1.5, 2.3 (Table 1).

Table 1 Composition of photopolymerizable resins MAPTMS/TiP/MAA

Resin	Molar ratio		Composition (mmol)						
	Molar ratio Ti/Si	Molar ratio H_2O/MAPTMS	MAPTMS	Acetone (MAPTMS)	HCl 0.1M	TiP	Acetone (TiP)	MAA	Michler's ketone
A	0.4	0.25	8.13	8.69	2.03	3.48	7.31	3.48	0.15
B	0.4	0.5	8.13	8.69	4.07	3.48	7.31	3.48	0.15
C	0.4	1	8.13	8.69	8.13	3.48	7.31	3.48	0.15
D	0.4	3	8.13	8.69	24.40	3.48	7.31	3.48	0.15
E	0.7	1	6.89	7.36	6.89	4.57	9.59	4.57	0.15
F	1	1	5.64	6.03	5.64	5.66	11.88	5.66	0.15
G	1.5	1	4.43	4.73	4.43	6.72	14.09	6.72	0.15
H	2.3	1	3.30	3.53	3.30	7.71	16.16	7.71	0.15

2.3 Photopolymerizable resins: MAPTMS/TiB/MAA

In an amber vial, the silicon precursor solution is prepared: a solution of MAPTMS at 80 wt% in acetone is prepared, and a solution of diluted HCl (0.1M) is added to hydrolyze the silane. The molar ratio H_2O/MAPTMS is maintained to 1 (Table 2). The reaction is stirred for one hour.
Simultaneously, in another amber vial, a solution of the titanium precursor is prepared. A solution of $Ti(OBu)_4$ (TiB) at 70 wt% in acetone is prepared and the MAA is added slowly under stirring, with a molar ratio equal to 1. The precise quantities are available in Table 2. The reaction is stirred for one hour.
Finally, the resin is prepared in a third amber vial. The silicon solution is added to the photoinitiator, Michler's ketone, (0.15 mmol). The titanium solution is dropped under stirring. The molar proportion of the TiB solution added to the MAPTMS solution is tuned, in the different samples, from 0 to 1. The exact quantities used for the resins are specified in Table 2.

Table 2 Composition of photopolymerizable resins MAPTMS/TiB/MAA

Resin	Molar ratio	Composition (mmol)						
	Molar ratio Ti/Si	MAPTMS	Acetone (MAPTMS)	HCl 0.1M	TiB	Acetone (TiB)	MAA	Michler's ketone
I	No Ti	13.81	14.76	13.81	0	0	0	0.15
J	0.4	8.70	9.30	8.70	3.73	9.37	3.73	0.15
K	0.7	7.21	7.70	7.21	4.82	12.10	4.82	0.15
L	1	5.84	6.24	5.84	5.82	14.61	5.82	0.15
M	1.5	4.47	4.78	4.47	6.82	17.12	6.82	0.15
N	2.3	3.30	3.53	3.30	7.67	19.26	7.67	0.15
O	No Si	0	0	0	10.08	25.31	10.08	0.15

2.4 Combined photopolymerizable and photobase resin

This resin (resin P) is adapted from the resin J in Table 2, by simply adding the photobase N-methylnifedipine ethyl ester derivative with the photoinitiator in the same experimental conditions.

In an amber vial, 8.70 mmol of MAPTMS are diluted with 9.30 mmol of acetone and 8.70 mmol of diluted HCl (0.1M) are added to hydrolyze the silane. The reaction is stirred for one hour.

Simultaneously, in another amber vial, 3.73 mmol of $Ti(OBu)_4$ (TiB) are dissolved in 9.37 mmol of acetone. 3.73 mmol of MAA are added slowly under stirring. The reaction is stirred for one hour. Finally, the resin is prepared in a third amber vial. The silicon solution is added to the photoinitiator, Michler's ketone, (0.15 mmol) and the photobase N-methylnifedipine ethyl ester derivative (0.41 mmol). The titanium solution is dropped under stirring. To ensure full solubilization of the photobase, 86 mmol of acetone are then added.

2.5 Two-photon lithography

The microfabrication setup (Microlight 3D) is based on an inverted microscope. The irradiation source is a Q-switched, frequency doubled Nd-YAG laser (532 nm, 12 kHz, 560 ps) focused by a microscope objective (Plan-Apochromat 40x/0.95, Zeiss) into the sample that is placed on a quartz cover slip (24 mm x 24 mm x 0.17 mm). During the microfabrication the focused laser spot is scanned through the trajectory defining the 3D microstructure to be printed, which is realized by varying the sample position by a piezo stage with respect to the focal spot. The microfabrication parameters such as 3D trajectory, laser power, exposure time are controlled by a dedicated software. For the microfabrication of structures with hybrid resins, the irradiation power is varied from 10 to 100 µW (measured at the entrance of the objective) and exposure time from 1 to 10 ms.

The sample is placed on a piezoelectric plate (PI Mars) also controlled via the dedicated software and allowing displacements of 100 µm in the 3 directions. The microstructure is divided into lines via modeling software, to obtain the layout of the fabrication. The laser and the piezo stage then follow the instructions of the software to create the microstructure.

To prepare the sample, a quartz microscope slide (24mmx24mmx0.17mm) is treated with an ultrasonic bath of a 5 wt% KOH solution in water for 10 minutes, then an ultrasonic bath of acetone for 5 minutes. Finally, it is dried under isopropanol vapor. A drop of 5 µL of resin is deposited on a quartz microscope slide substrate and is left for aging before performing the fabrication. Three aging times of 1h, 1h30 and 2h have been considered. Microfabrication is carried out on the surface of the quartz slide. Once the fabrication is complete, the substrate is removed from the instrumentation to be washed in an acetone bath for 5 minutes, in order to remove the excess of unreacted resin and reveal the microstructures fabricated by two-photon lithography.

2.6 Pyrolysis process

The microfabricated structures are calcined in an alumina crucible directly on their quartz substrates using a muffle furnace (Thermolyne FB1300, Thermo Scientific) without particular airflow regulation. For the structures calcined at 600°C, a temperature ramp of 5°C/min is applied up to 600°C, and this temperature is maintained for 30 minutes before allowing the oven to cool down to room temperature without any particular control. For the structures calcined at 1000°C, a temperature ramp of 5°C/min is applied up to 1000°C, and this temperature is maintained for 60 minutes before allowing the oven to cool down to room temperature without any particular control.

2.7 FTIR spectroscopy

For each resin, a drop of 5 µL is deposited onto a glass slide, in order to form a film. An aging time of 1h is fulfilled and the measure is conducted using a FTIR spectrometer equipped with an ATR device from PerkinElmer (Spectrum65). The background due to the glass slide is recorded and directly subtracted from the obtained signal. Then the films are exposed to UV light (255nm; 20µW/cm^2) for 15 minutes, in order to polymerize the material, and a second measure is performed. The FTIR spectra were performed from 550 to 4000 cm^{-1} and are presented as obtained without any post treatment.

2.8 SEM observations

The microstructures are sputtered with a 5 nm layer of platinum using a high vacuum coater (EM ACE600, Leica) and observed with SEM (Supra55VP, Zeiss) at a beam of 10 kV, through a secondary electron detector.

2.9 XRD experiments

The resins are exposed to UV light (255nm; 20µW/cm^2) for 2 hours, until a solid is formed. The materials are crushed in fine powders in a mortar. They are then calcined as described in the pyrolysis process and the diffractograms are recorded after the heating treatment at 600°C and 1000°C. The diffractograms are performed from 10° to 80° (2theta) but they are presented here from 10° to 65° where the structural information is located. The diffractograms were post-treated to adjust the background and to smoothed the lines.

2.10 MicroRaman spectroscopy

The microRaman instrument allows analyzing directly the microstructures, with a focalization of the laser through a microscope objective, on a precise location of the micro-object, without further preparation. The micro Raman analyses were conducted with a Horiba LabRamn HR evolution spectrometer. In backscattering geometry, the excitation laser (532 nm) was focused and the Raman diffusion was collected through the same objective (x100/0.9 Olympus). The materials based on the MAPTMS/TiB/MAA resins are characterized.
Microgrids of 50 µm are fabricated by two-photon lithography for different molar ratios Ti/Si with TiB and calcined according to the pyrolysis process. Microfabrication of the resin O (No Si) is not achievable therefore a drop of the resin is deposited onto a quartz substrate and calcined according to the pyrolysis process. The probe size of the device is lower than 1 µm that is adapted to a precise localization on the microstructure, so Raman spectra are obtained at this precise position. The green point on Fig. 2 allows to figure out the position of laser on the grid.

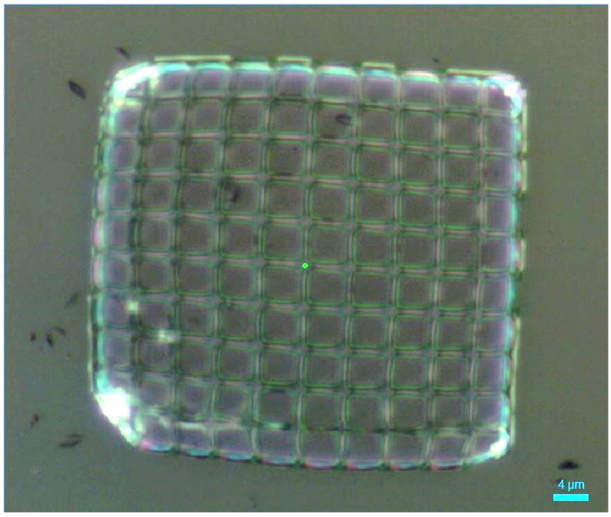

Fig. 2 Example of microgrid obtained with resin J observed with the x100 objective of the microRaman set-up. The green dot is the analyzed location

Each spectrum is collected with 5 accumulations of 20 second of acquisition. The useful structural information is located in the wavenumber range from 200 to 1000 cm^{-1}. As for different locations, it appears that the microstructures are very homogenous, the spectra have not been processed and are presented as measured.

3 Results and discussion

3.1 Influence of the titanium precursors on the microfabrication process

The first resin MAPTMS/TiP/MAA, used as a comparative reference, is similar to those realized in a previous study [10]. The maximum of molar ratio Ti/Si is 1 and at this concentration, the microfabrication is limited and the microstructures surface is often rough. The conditions of the preparation of the resins are varied and microgrids are realized using two-photon lithography to observe the difference in resolution on the linewidth of the structures (Fig. 3 (a)). The common definition for the resolution of microstructures fabricated by two-photon lithography is the minimum distance between the centers of two lines without overlapping between them [28]. Here, as a simplified approach, a simple measure of the linewidth is performed.

With the resin MAPTMS/TiP/MAA, as in the previous study, no fabrication above a molar ratio Ti/Si of 1 is observed and at this concentration, the structures are stiff and present cracks. In the second resin, the titanium precursor, i.e. the titanium isopropoxide, is replaced by a more sterically hindrance precursor, the titanium butoxide. The modified alkoxide is more stable and allows fabrication up to a molar ratio Ti/Si of 2.3. Moreover, the microgrids obtained with TiB give more resolved structures that break less easily (Fig. 3 (b)).

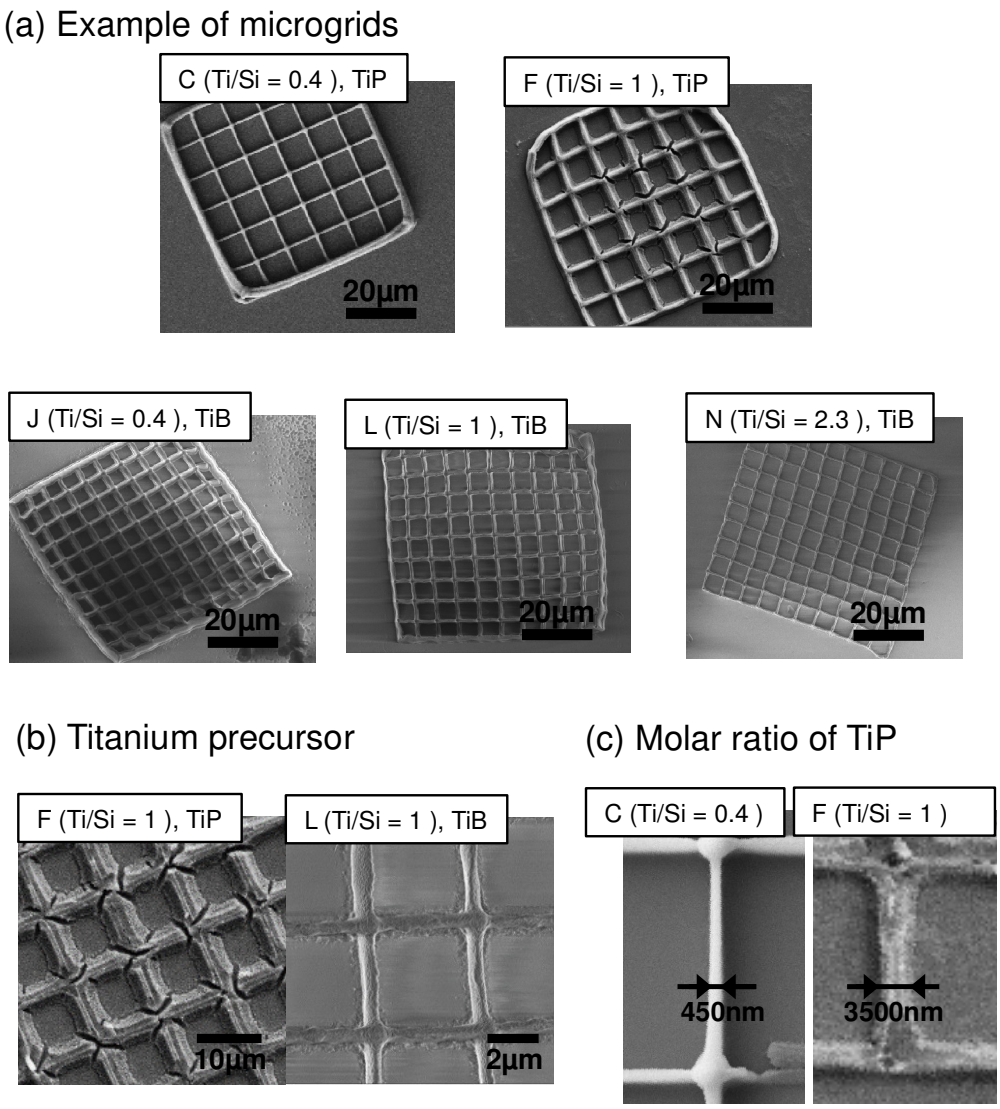

Fig. 3 (a) Example of microgrids obtained from resins at different molar ratios Ti/Si with TiP and TiB (resins C, F, J, L, N) (b) Comparison between microlines obtained from resins with TiP and TiB, printed at 70µW, after an aging time of 1h (resins F, L) (c) Microlines obtained at 70µW from resins at different molar ratios Ti/Si with TiP, after an aging time of 1h (resins C, F)

For both resins, when the titanium content increases, the linewidth increases and the reaction spreads in an uncontrolled way far away from the focal point, inducing a loss of resolution, as shown in Fig. 3 (c). For an important ratio of Ti, the fabrication is jeopardized. It is thus not possible to obtain results from the resin G and H, which corresponds to a molar ratio Ti/Si of 1.5 and 2.3 with TiP. In addition, the fabrication threshold is strongly lowered, so less energy is needed to initiate the microfabrication process. For example, the microfabrication threshold for

resin I (No Ti) is around 2.5 mW whereas for the resin N (molar ratio Ti/Si = 2.3) the threshold is only around 50 µW, which is 50 times more sensitive. Moreover, observations show that the titanium butoxide allows a better stability of the resin than titanium isopropoxide, consequently leading to a higher polymerization threshold (Table 3).

Table 3 Observations of the stability of the resins (storage at 4°C, sheltered from light) and polymerization thresholds

Resin	Molar ratio Ti/Si	Stability	Polymerization threshold
I	No Ti	More than 3 months	~2.5 mW
C	0.4 (TiP)	2 months	~50 µW
E	0.7 (TiP)	1 month	ND
F	1 (TiP)	2 weeks	~30 µW
G	1.5 (TiP)	1 week	No fabrication
H	2.3 (TiP)	1 week	No fabrication
J	0.4 (TiB)	More than 3 months	~70 µW
K	0.7 (TiB)	More than 3 months	ND
L	1 (TiB)	2 months	~60 µW
M	1.5 (TiB)	2 weeks	ND
N	2.3 (TiB)	1 week	~50 µW
O	No Si (TiB)	2 days	No fabrication

3.2 Influence of experimental conditions on the microfabrication with MAPTMS/TiP/MAA

The photopolymerizable resin is obtained following basically a three-steps procedure, (i) the hydrolysis of the MAPTMS, (ii) mixing of the precursors and (iii) the sol-gel aging. Then it is possible to perform the two-photon polymerization and have the final micro-object. These key parameters of the process are varied in order to evaluate the incidence on the microfabrication resolution.

First the hydrolysis ratio of MAPTMS with in acidic medium (HCl) is investigated (molar ratio H_2O/MAPTMS = 0.25, 0.5, 1 and 3 – corresponding to the resins A, B, C and D) to evaluate the

influence on the overall process. After an aging time fixed to 1h, microgrids are patterned with a laser power of 70µW (exposition time 5ms) and the width of the printed lines is determined from the SEM images (Fig. 4 (a)). The resolutions obtained for a molar ratio H_2O/MAPTMS of 0.25, 0.5 and 1 are compared. The best resolutions are obtained with a ratio of 0.5 and the results are surprisingly not linear. For a ratio of 3, which is the condition of total hydrolysis (resin D), the material is formed but we observe that it swells almost immediately. There is an optimal molar H_2O/MAPTMS ratio to balance the hydrolysis/condensation and the polymerization reactions.

Before starting the process of the microfabrication, an aging time is respected. During this time, the solvent starts to evaporate and the sol-gel condensation occurs in order to pre-form the hybrid network. The influence of this parameter is investigated and appears to have a major impact in the control of the linewidth of fabricated objects. Microgrids are fabricated from the resin B with a laser power of 70µW (exposition time 5 ms) after three different aging times of 1h, 1h30 and 2h. The widths of the lines are estimated from SEM images (Fig. 4 (b)). The SEM images show that when the aging time increases, inducing higher condensation ratio, the linewidth is increasing too and the resolution is lost.

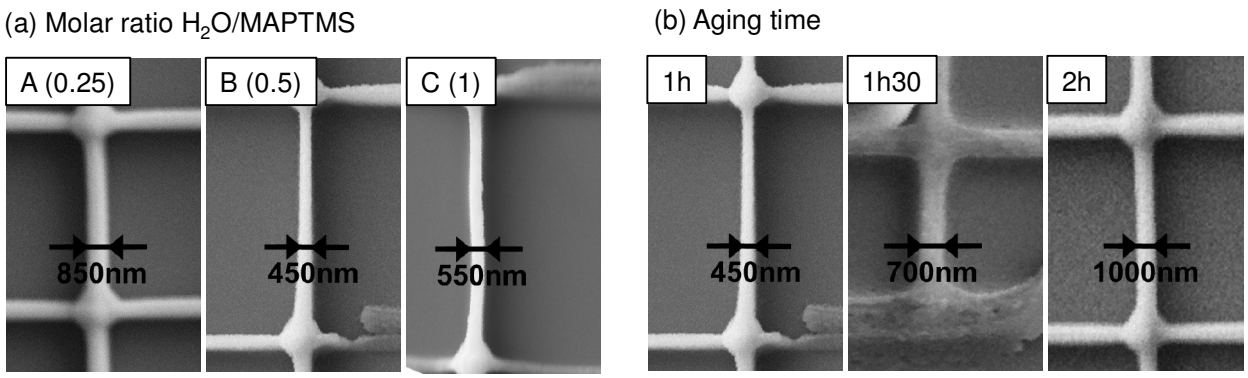

Fig. 4 Microlines printed at 70µW, obtained from resins in function of different experimental preparation conditions (a) Variation of molar ratio H_2O/MAPTMS, after an aging time of 1h (resins A, B and C) (b) Variation of aging time (resin B)

3.3 Addition of the photobase towards simultaneous two-photon sol-gel condensation and polymerization

The mechanism for the lithography of the hybrid resins implies two chemical reactions in two steps: sol-gel condensation followed by radical photopolymerization. The aging step to provoke the sol-gel condensation is essential but requires time. A recent study by our group has highlighted the possibility to photo-induce the sol-gel condensation by activating a photobase present in a sol-gel resin [14, 15]. This photobase is added to typical formulation of a hydrid resin (resin P) in order to simultaneously perform the two polymerization steps required for the lithography of the hybrid resins. No improvement of resolution is observed during the microfabrication process as well as the power required for obtaining microstructure is a little higher: 0.07 V are required for the resin P (in presence of the photobase) instead of 0.05 V necessary for the resin J (without the photobase). Finally, at this stage in our experimental conditions, the combination of photobase and photinitiator do not allow improvement the process but the system deserves to be further explored.

3.4 Characterization of MAPTMS/TiB/MAA resins by FTIR spectroscopy

Films of MAPTMS/TiB/MAA resins containing the different molar ratios Ti/Si with TiB are characterized by FTIR spectroscopy in order to investigate the different reactions involved during the microfabrication process. For the sol-gel condensation reaction, the elongation band of OH groups at 3500 cm^{-1} is an indication of the quantity of silanol groups available to condense and form photoreactive clusters. For the radical photopolymerization, the representative elongation band of C=C bond at 1640 cm^{-1} is known to decrease during the process of polymerization.
Fig. 5 shows the evolution of the elongation band of the OH groups around 3500 cm^{-1} as a function of the molar ratio Ti/Si after an aging time of 1 hour. It appears that this band is reducing with the increase of Ti amount. The condensation ratio is nearly total for the resin O (No Si) while numerous silanol groups are remaining for the resin I (No Ti), indicating that the Ti is more sensitive to the condensation as expected, and favoring also the condensation of the silanol groups.

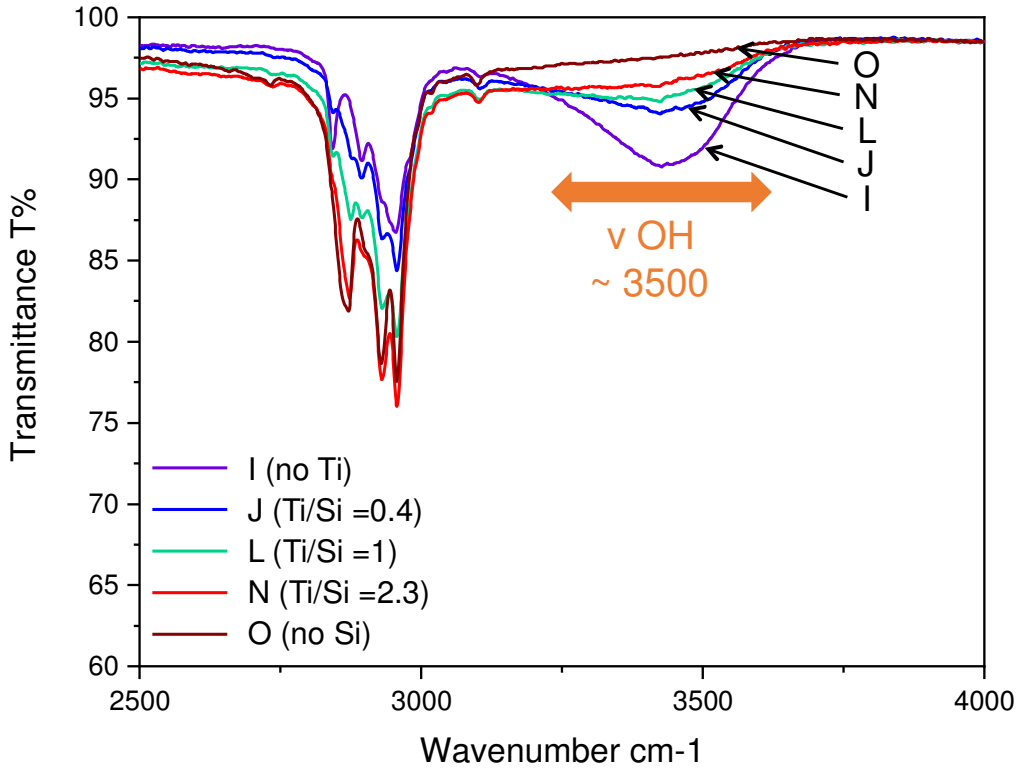

Fig. 5 IR spectra of films for different molar ratios Ti/Si (resins I, J, L, N, O), focusing on the OH elongation band at 3500 cm^{-1}

Fig. 6 shows the FTIR spectra of these films before and after a 1 photon excitation through an exposure to UV light (255 nm), for different molar ratios Ti/Si. The spectral observation zone is reduced to reveal the elongation of C=C at 1640 cm^{-1}. This corresponds to the acrylate functions present on the MAA and the MAPTMS, supposed to decrease under UV exposure while the radical photopolymerization of the acrylate being achieved. In such UV exposure conditions, for the resin I (no Ti), no radical photopolymerization occurs. At the same time the sol-gel condensation is not achieved. In contrast, for the for the resins J and N, containing mixtures of Si

and Ti precursors, the radical photopolymerization is efficient, as indicated by the decrease of the C=C band. At the same time the condensation of silanol groups is ongoing. For the resin O (no Si), the radical photopolymerization is not as efficient and at the same time, the condensation is nearly total. The advancement of the sol-gel condensation, leading to the formation of photoreactive clusters, is influencing the efficiency of the radical photopolymerization.

During the microfabrication, the reaction becomes more sensitive when the titanium precursor content increases. The FTIR results show that the increase of Ti leads to a higher condensation ratio and eventually to a complete condensation. The results also show that the radical photopolymerization is favored in presence of Ti but inhibited in case of complete condensation. Thus, the organic reaction strongly depends on the inorganic reaction.

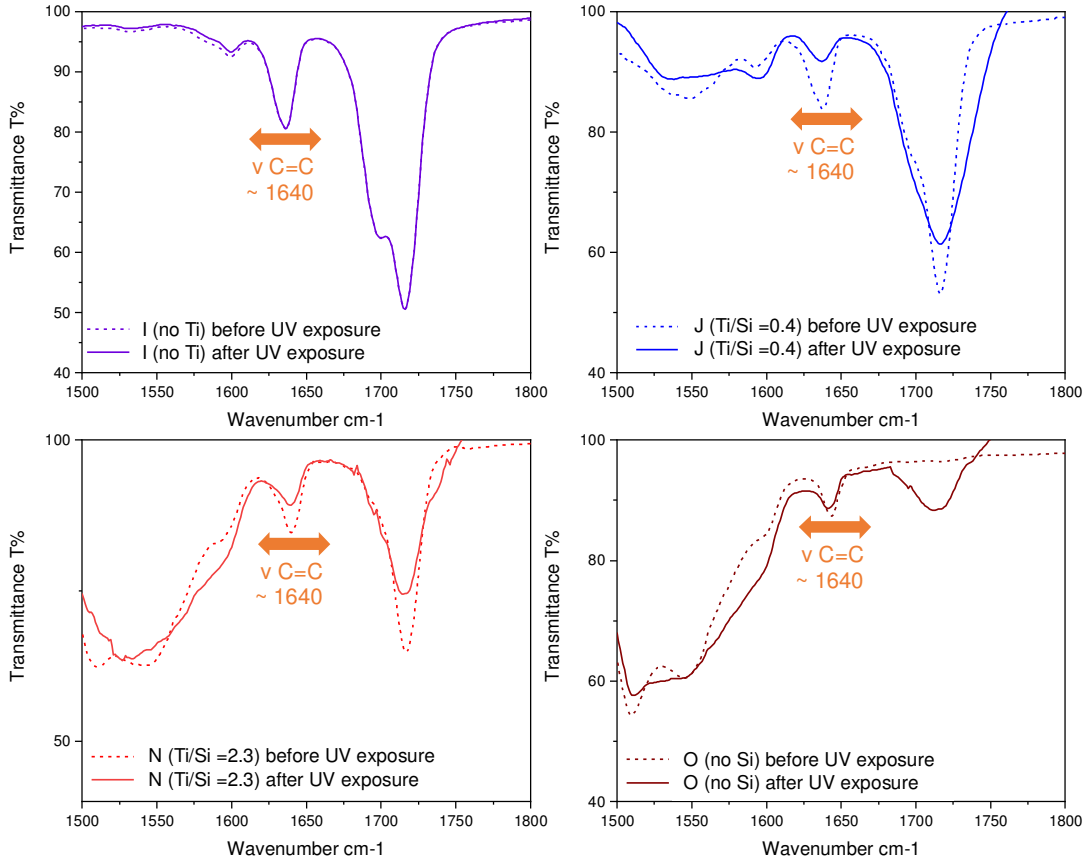

Fig. 6 IR spectra on films with different molar ratios Ti/Si (resins I, J, N, O) before and after UV exposure, focusing on the C=C elongation band at 1640 cm^{-1}

The chemical process implemented during the microfabrication implies thus a double polymerization either sequential or simultaneous. The sol-gel condensation forms a network of photoreactive clusters (inorganic condensation), which is consolidated by the radical photopolymerization (organic polymerization). The presence and quantity of the titanium precursor has a significant role in the execution of these reactions and their respective kinetics. It increases the part devoted to the inorganic condensation reaction in competition with the organic photopolymerization, and as a consequence the microfabrication becomes more difficult to control. Regarding the simultaneous two-photon sol-gel condensation and polymerization process adding the photobase, the radical polymerization is still efficient in presence of the photobase, but no notable influence is observed regarding the sol-gel condensation (Fig. 7).

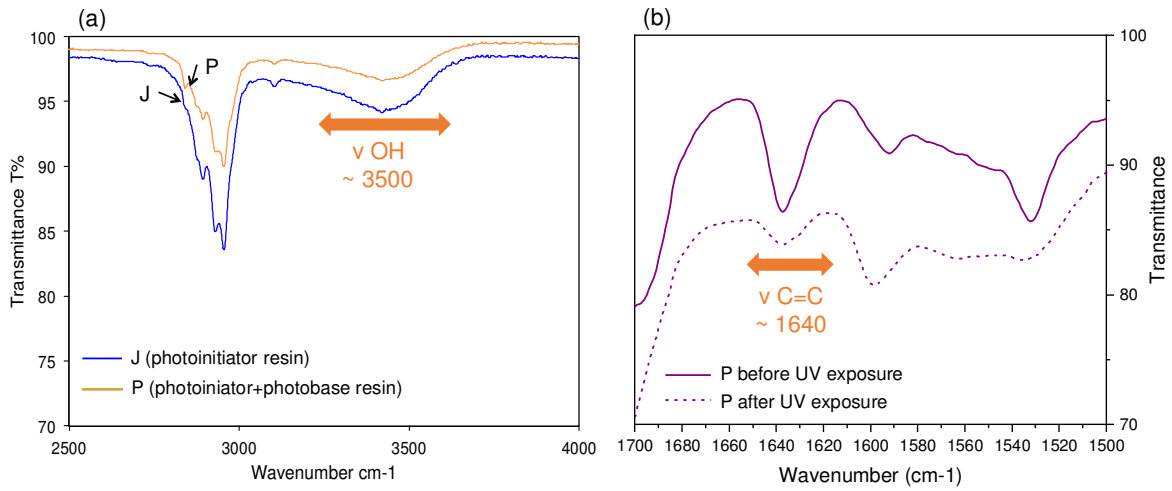

Fig. 7 (a) IR spectra on films of the photobase resin (resin P) and the photoinitiator resin (resin J) as reference, focusing on the OH elongation band at 3500 cm^{-1} (b) IR spectra on films of the photobase resin (resin P) before and after UV exposure, focusing on the C=C elongation band at 1640 cm^{-1}

3.5 Pyrolysis of microgrids towards the ceramics: X-ray diffraction and microRaman

Pyrolysis of microstructures with different molar ratios Ti/Si are achieved in order to obtain ceramics from the hybrid structures. The debinding of the organic part irremediably leads to the

shrinkage of the microstructures up to 50% (Fig. 8). This phenomenon was previously observed but usually leads to collapse of the ceramic structure [29].

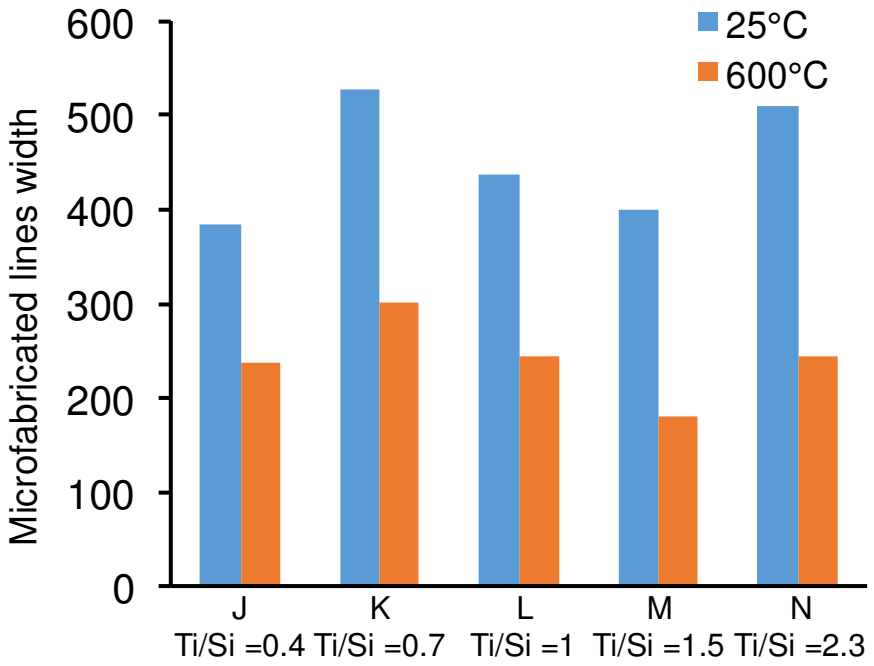

Fig. 8 Linewidths of microgrids obtained from resins at different molar ratios Ti/Si before and after pyrolysis

The pyrolyzed microstructures are characterized by XRD and microRaman analyses. XRD experiments are not performed directly on the microstructures, but on bulk materials. The microRaman experiments are performed directly on the printed microstructures. The combined results of these characterizations provide important information on the ceramic phases obtained after the pyrolysis.

The XRD results (Fig. 9 and Fig. 10) show that when the ratio of Ti increases, the formation of titanium dioxide phases is favored for both pyrolysis temperatures. At 600°C, the diffractograms show that the samples are only partially crystalline, whereas at 1000°C the crystallinity is better for all compositions. At 600°C, for the sample O (no Si), a mixture of anatase and rutile phases is obtained, whereas at 1000°C, the pure rutile is observed. That is in adequacy with several reports [30, 31].

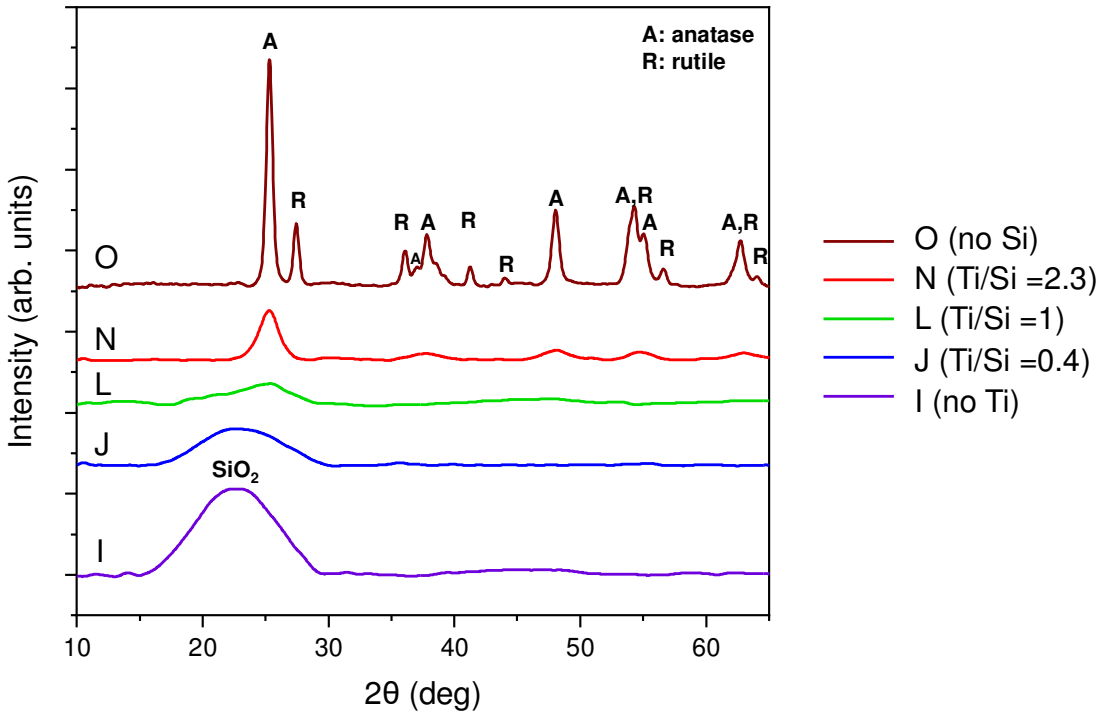

Fig. 9 X-ray diffractograms of materials obtained from resins at different molar ratios Ti/Si (resins I, J, L, N, O) after pyrolysis at 600°C

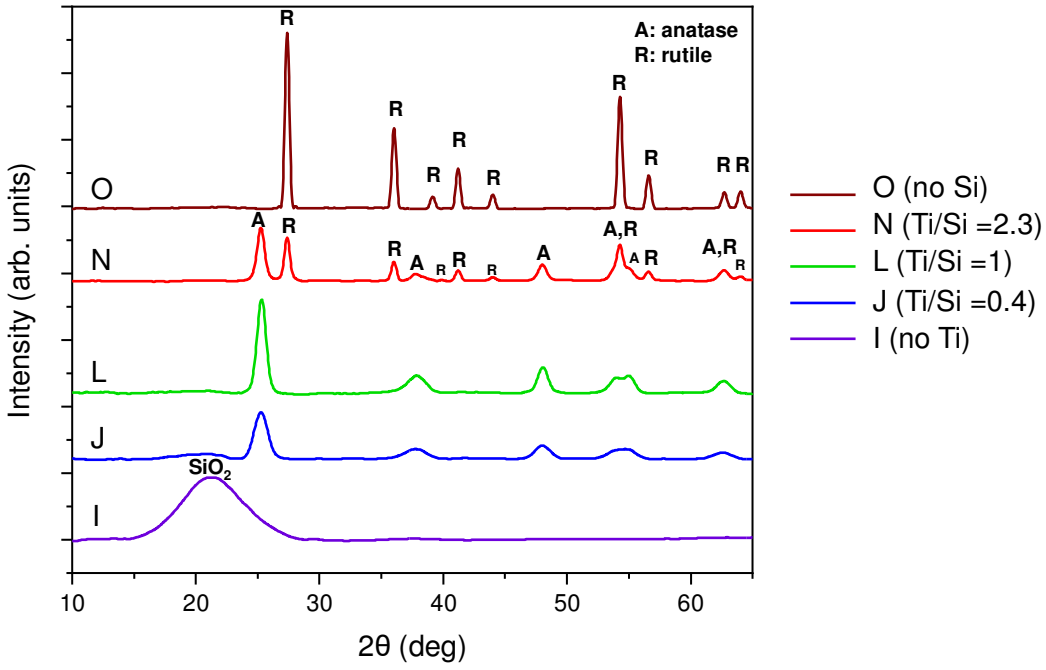

Fig. 10 X-ray diffractograms of materials obtained from resins at different molar ratios Ti/Si (resins I, J, L, N, O) after pyrolysis at 1000°C

The microRaman spectroscopy is a useful tool to characterize objects at the microscale. MicroRaman analyzes are performed directly on the microfabricated grids on materials prepared at different molar ratio Ti/Si. Two pyrolysis temperature are considered, 600°C and 1000°C. Before the pyrolysis, the system is partially organic whereas after the calcination, the presence of a mixture of TiO_2 and SiO_2 is observed in line with XRD experiments and previous reports [32, 33]. It demonstrates that the ceramics obtained by the process of microfabrication followed by pyrolysis show the same crystallographic phases as those obtained from bulk samples. So, the process of fabrication has no influence on the obtained crystalline phases.

After the pyrolysis at 600°C (Fig. 11), a mixture of anatase and rutile crystalline TiO_2 is observed. The typical band of titanium dioxide anatase at 141, 197, 395, 517 and 638 cm^{-1}, titanium dioxide rutile at 145, 445 and 610 cm^{-1}, and fused silica at 490 cm^{-1} are observed [34, 35]. The full indexation of the Raman bands is provided in Table 4. The typical pattern of fused silica, with a large band at 490 cm^{-1}, is observable for the sample I (no Ti). For low ratios of

titanium, the bands of the anatase are still present but less intense, broader and eventually shifted. For example, the band at 141 cm^{-1} is shifted to 150 cm^{-1} with a molar ratio of 1.5 (sample M) in presence of Si in the material. For the mixed SiO_2/TiO_2 material, the bands are very broad, indicating the materials have probably an amorphous part. The origin of the band at 550 cm^{-1} is not clear. This can be tentatively attributed to either the possible formation of titanium carbide during the pyrolysis, or artifacts due to surface effects [36].

After the pyrolysis at 1000°C (Fig. 12), more crystallized phases are obtained. The same typical band of anatase, rutile and fused quartz are observed and indexed in Table 4. Regarding the sample O (no Si), the phase transition from a rutile and anatase mixture at 600°C to the pure rutile phase at 1000°C is noted, being consistent to XRD experiments. The materials containing mixtures of Si and Ti present systematically a mixture between rutile and anatase phases, with the trend to form more rutile when the titanium amount increases. The presence of silicon limits the formation of rutile, for the benefit of the anatase phase. Note that the Raman band due to SiO_2 is covered by the presence of the titanium dioxide phases.

The combined XRD and microRaman experiments bring important information on the material formed during the pyrolysis. The temperature of the pyrolysis has an influence on the ceramic phase obtained. At 600°C, the anatase Titania is formed whereas at 1000°C, the rutile phase appears. The signal due to SiO_2 is reduced when the molar ratio Ti/Si increases, confirming so a higher content of titanium.

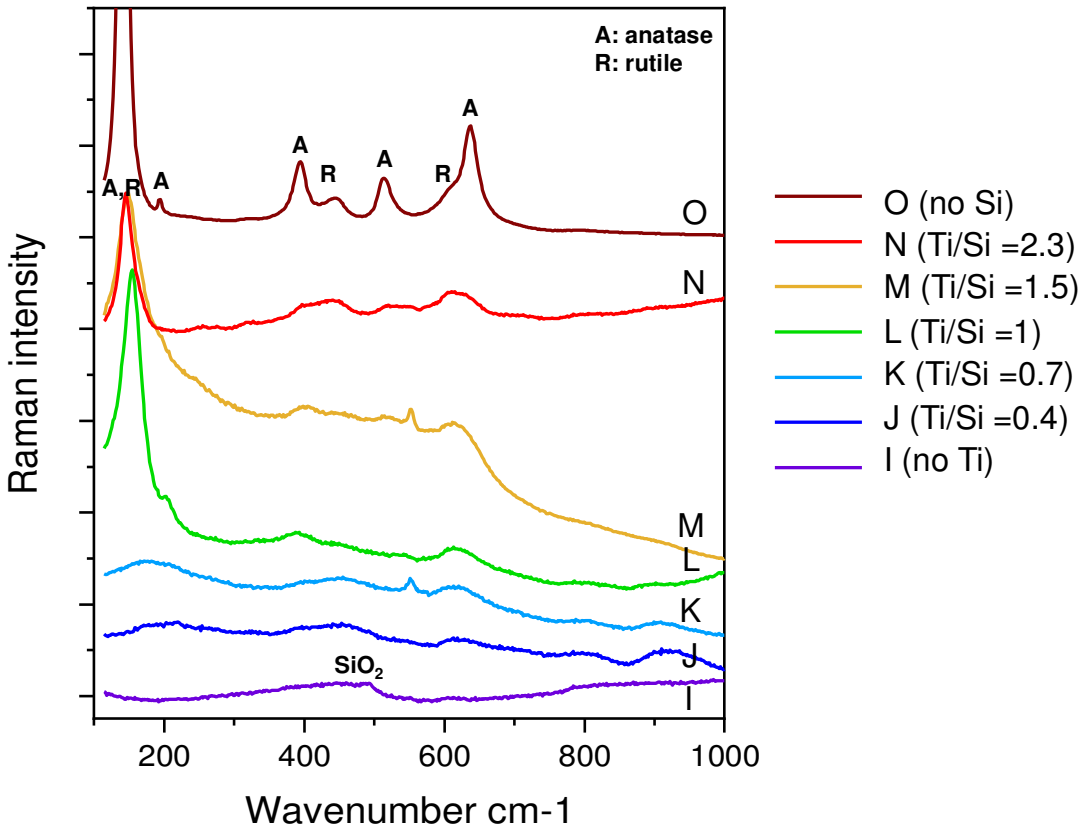

Fig. 11 Raman spectra of materials obtained from resins at different molar ratios Ti/Si (resins I, J, K, L, M, N, O) after pyrolysis at 600°C

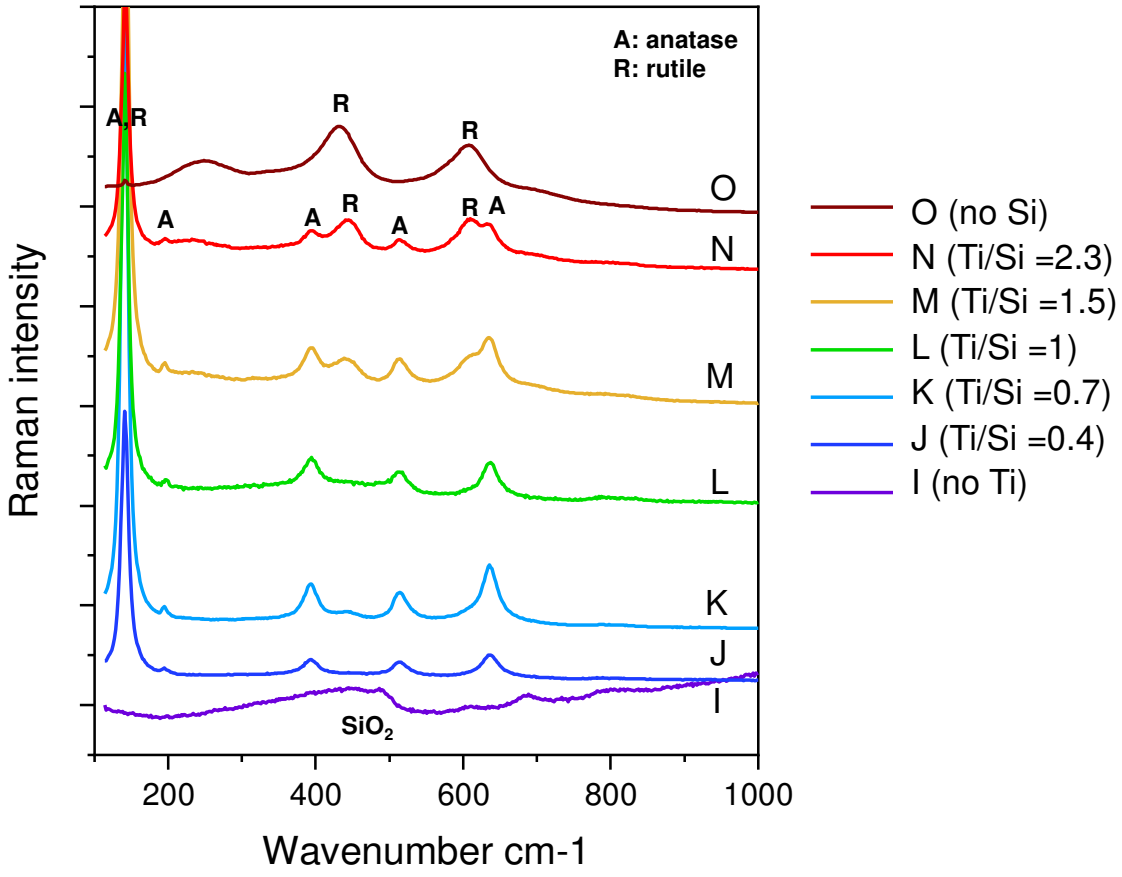

Fig. 12 Raman spectra of materials obtained from resins at different molar ratios Ti/Si (resins I, J, K, L, M, N, O) after pyrolysis at 1000°C

Table 4 Indexation of the Raman bands observed of materials obtained from resins at different molar ratios Ti/Si (resins I, J, K, L, M, N, O) after pyrolysis at 600°C (top) and 1000°C (down)

600°C	I	J	K	L	M	N	O
Molar ratio	No Ti	0.4	0.7	1	1.5	2.3	No Si
Mode E_g anatase		200	180	160	150	141	141
Mode B_{1g} rutile							141
Mode E_g anatase				195			195
Mode B_{1g} anatase				396	396	396	396
Mode E_g rutile					445	445	445
Fused quartz	490	490	490				
Mode A_{1g}+B_{1g} anatase					516	516	516
Mode A_{1g} rutile		616	616	616	616	610	608
Mode E_g anatase		640	640	640	640	640	640

1000°C	I	J	K	L	M	N	O
Molar ratio	No Ti	0.4	0.7	1	1.5	2.3	No Si
Mode E_g anatase		141	141	141	141	141	
Mode B_{1g} rutile							143
Mode E_g anatase		195	195	195	195	195	
Mode B_{1g} anatase		396	396	396	396	396	
Mode E_g rutile					445	445	440
Fused quartz	490						
Mode A_{1g}+B_{1g} anatase		516	516	516	516	516	
Mode A_{1g} rutile					611	611	608
Mode E_g anatase		640	640	640	640	640	

By combining XRD and microRaman experiments, we prove the capacity of the initial inorganic-organic material to transform to a ceramic material composed of SiO_2/TiO_2 through the pyrolysis and thus to obtain ceramic materials from the two-photon lithography.

4 Conclusion

In this paper, the possibility of obtaining microceramics by two-photon fabrication and pyrolysis is demonstrated. The deep investigation in the process parameters highlights the importance of controlling the hydrolysis/condensation parameters of the sol-gel reaction versus the polymerization for the control of the microfabrication of hybrid resins and the resolution of the printed materials. Traditionally, photoinduced free-radical polymerization of acrylate monomers is the driving phenomena of the two-photon fabrication processes. In this case there is a double polymerization process. On the one hand, the inorganic part obtained by the sol-gel reaction, during which the alkoxide precursors hydrolyze and condense. On the other hand, the organic polymerization takes part, which binds the oligomers formed by sol-gel reactions and thus finalize the microfabrication process through the double cross-linking. The impact of the inorganic reaction on the resolution and the organic polymerization threshold is crucial. The aging step is thus to be considered before the microfabrication. In particular, this step strongly impacts the polymerization threshold, opening the possibilities to improve the final resolution compared to pure organic polymeric systems. The influence of the choice of titanium precursor is also highlighted, indeed the use of titanium butoxide instead of titanium isopropoxide allows increasing the molar ratio Ti/Si from 1 to 2.3 and so to increase the titanium amount in the final composite microstructures. By performing the pyrolysis of the two-photon fabricated microstructures, it is possible to obtain TiO_2 based micro-ceramics, identifiable by XRD and microRaman analyses, and thus to obtain microstructures with optical, electronic and mechanical properties that are potentially much more interesting.

Acknowledgement

The authors are grateful to the European Union's Horizon 2020 research and innovation program PHENOmenon under grant agreement nº 780278 for funding and to the Raman facility in Lyon (France) supported by the Institut National des Sciences de l'Univers (INSU) and the "Programme National de Planétologie". This is a contribution of the LABEX Lyon Institute of Origins (ANR-10-LABX-0066), within the program "Investissements d'Avenir" (ANR-11-IDEX-0007) at Université de Lyon. The region Auvergne-Rhône-Alpes is acknowledged for the partial funding through the IRICE project 3DFAB.

References

1. Zaouk R, Park BY, Madou MJ (2005) Introduction to Microfabrication Techniques, in *Microfluidic Techniques*, New Jersey: Humana Press, 321:3

2. Park SG, Jeon TY, Yang SM (2013) Fabrication of 3D Nanostructured Titania Materials by Prism Holographic Lithography and the Sol-Gel Reaction. Langmuir 29(31):9620. doi: 10.1021/la4023163

3. Lim SH, Saifullah MSM, Hussain H, Loh WW, Low HY (2010) Direct imprinting of high resolution TiO_2 nanostructures. Nanotechnology 21(28):285303. doi: 10.1088/0957-4484/21/28/285303

4. Maruo S, Nakamura O, Kawata S (1997) Three-dimensional microfabrication with two-photon-absorbed photopolymerization. Opt Lett 22(2):132. doi: 10.1364/OL.22.000132

5. Wang I, Bouriau M, Baldeck P, Martineau C, Andraud C (2002) Three-dimensional microfabrication by two-photon-initiated polymerization with a low-cost microlaser. Opt lett 27:1348. doi: 10.1364/OL.27.001348

6. Sun HB, Kawata S (2004) Two-Photon Photopolymerization and 3D Lithographic Microfabrication , APS 170:169. doi: 10.1007/b94405

7. Farsari M, Chichkov B (2009) Two-photon fabrication, Nature Photonics 3:450. doi: 10.1038/nphoton.2009.131

8. Ostendorf A, Chichkov B (2006) Two-photon polymerization: A new approach to micromachining. Photonics Spectra 40:72

9. Serbin J, Egbert A, Ostendorf A, Chichkov B, Houbertz R, Domann G, Schulz J, Cronauer C, Fröhlich L, Popall M (2003) Femtosecond laser-induced two-photon polymerization of inorganic–organic hybrid materials for applications in photonics. Opt Lett 28:301–303. doi: 10.1364/OL.28.000301

10. Sakellari I, Gaidukeviciute A, Giakoumaki A, Gray D, Fotakis C, Farsari M, Vamvakaki M., Reinhardt C, Ovsianikov A, Chichkov BN (2010) Two-photon polymerization of titanium-containing sol–gel composites for three-dimensional structure fabrication. Appl Phys A 100(2):359. doi: 10.1007/s00339-010-5864-0

11. Ovsianikov A, Gaidukeviciute A, Chichkov BN, Oubaha M, MacCraith BD, Sakellari I, Giakoumaki A, Gray D, Vamvakaki M, Farsari M, Fotakis C (2008) Two-Photon Polymerization

of Hybrid Sol-Gel Materials for Photonics Applications. Laser Chemistry 2008: 493059. doi: 10.1155/2008/493059

12. Ovsianikov A, Viertl J, Chichkov B, Oubaha M, MacCraith B, Sakellari I, Giakoumaki A, Gray D, Vamvakaki M, Farsari M, Fotakis C (2008) Ultra-Low Shrinkage Hybrid Photosensitive Material for Two-Photon Polymerization Microfabrication. ACS Nano 2(11):2257. doi: 10.1021/nn800451w

13. Vyatskikh A, Delalande S, Kudo A, Zhang X, Portela CM, Greer JR (2018) Additive manufacturing of 3D nano-architected metals. Nat Commun 9:593. doi: 10.1038/s41467-018-03071-9

14. Kustra J (2018) Elaboration of micro and mesostructured sol-gel materials using polysilsesquioxane molecular precursors. PhD thesis, Lyon, France and Krakow, Poland

15. Kustra J, Martin E, Chateau D, Lerouge F, Monnereau C, Andraud C, Sitarz M, Baldeck PL, Parola S (2017) Two-photon controlled sol–gel condensation for the microfabrication of silica based microstructures. The role of photoacids and photobases. RSC Adv 7(74):46615. doi: 10.1039/C7RA08608C

16. Lim TW, Son Y, Yang D-Y, Pham TA, Kim DP, Yang BI, Lee KS, Park SH (2008) Net Shape Manufacturing of Three-Dimensional SiCN Ceramic Microstructures Using an Isotropic Shrinkage Method by Introducing Shrinkage Guiders. International Journal of Applied Ceramic Technology 5:258–264. doi: 10.1111/j.1744-7402.2008.02234.x

17. Gailevičius D, Padolskytė V, Mikoliūnaitė L, Šakirzanovas S, Juodkazis S, Malinauskas M (2019) Additive-manufacturing of 3D glass-ceramics down to nanoscale resolution. Nanoscale Horiz 4:647–651. doi: 10.1039/C8NH00293B

18. Eckel ZC, Zhou C, Martin JH, Jacobsen AJ, Carter WB, Schaedler TA (2016) Additive manufacturing of polymer-derived ceramics. Science 351:58–62. doi: 10.1126/science.aad2688

19. Enyashin AN, Seifert G (2005) Structure, stability and electronic properties of TiO2 nanostructures. physica status solidi (b) 242:1361–1370. doi: 10.1002/pssb.200540026

20. Tang H, Prasad K, Sanjinès R, Schmid PE, Lévy F (1994) Electrical and optical properties of TiO2 anatase thin films. Journal of Applied Physics 75:2042–2047. doi: 10.1063/1.356306

21. Declerck P, Houbertz R, Jakopic G, Passinger S, Chichkov B (2007) High Refractive Index Inorganic-Organic Hybrid Materials for Photonic Applications. MRS Online Proceedings Library Archive 1007. doi: 10.1557/PROC-1007-S01-02

22. Yu SY, Schrodj G, Mougin K, Dentzer J, Malval JP, Zan HW, Soppera O, Spangenberg A (2018) Direct Laser Writing of Crystallized TiO_2 and TiO_2/Carbon Microstructures with Tunable Conductive Properties. Adv Mater 30(51):1805093. doi: 10.1002/adma.201805093

23. Psycharakis S, Tosca A, Melissinaki V, Giakoumaki A, Ranella A (2011) Tailor-made three-dimensional hybrid scaffolds for cell cultures. Biomed Mater 6:045008. doi: 10.1088/1748-6041/6/4/045008

24. Balčiūnas E, Baldock SJ, Dreižė N, Grubliauskaitė M, Coultas S, Rochester DL, Valius M, Hardy JG, Baltriukienė D (2019) 3D printing hybrid organometallic polymer-based biomaterials via laser two-photon polymerization. Polymer International 68:1928–1940. doi: 10.1002/pi.5909

25. Rozes L, D'Arras L, Hoffman C, Potier F, Halttunen N, Nicole L (2015) Titania-Based Hybrid Materials: From Molecular Precursors to the Controlled Design of Hierarchical Hybrid Materials, in Chemistry of Organo-Hybrids, John Wiley & Sons, Ltd, 114

26. Schubert U (2005) Chemical modification of titanium alkoxides for sol–gel processing. J Mater Chem 15(35□36):3701. doi: 10.1039/B504269K

27. Schubert U (2004) Organofunctional Metal Oxide Clusters as Building Blocks for Inorganic-Organic Hybrid Materials. J Sol-Gel Sci Technol 31(1):19. doi: 10.1023/B:JSST.0000047954.70820.dd

28. Baldacchini T (2015) Three-Dimensional Microfabrication Using Two-Photon Polymerization: Fundamentals, Technology, and Applications. William Andrew

29. Yee DW, Lifson ML, Edwards BW, Greer JR (2019) Additive Manufacturing of 3D-Architected Multifunctional Metal Oxides. Advanced Materials 31:1901345. doi: 10.1002/adma.201901345

30. Lee DH, Choi SY (2004) Preparation of photocatalytic TiO_2–SiO_2 thin film by sol-gel coating. Met Mater Int 10(4):357. doi: 10.1007/BF03185985

31. Lin YH, Weng CH, Srivastav AL, Lin YT, Tzeng JH (2015) Facile Synthesis and Characterization of N-Doped TiO_2 Photocatalyst and Its Visible-Light Activity for Photo-Oxidation of Ethylene. J Nanomat 807394. doi.org/10.1155/2015/807394

32. Bahtat M, Mugnier J, Bovier C, Roux H, Serughetti J (1992) Waveguide Raman spectroscopy of TiO_2:SiO_2 thin films. J Non-Cryst Solids 147:123. doi: 10.1016/S0022-3093(05)80604-0

33. Best MF, Condrate RA (1985) A raman study of TiO_2-SiO_2 glasses prepared by sol-gel processes. J Mater Sci Lett 4(8):994. doi: 10.1007/BF00721102

34. Ohsaka T, Izumi F, Fujiki Y (1978) Raman spectrum of anatase, TiO2. Journal of Raman Spectroscopy 7:321–324. doi: 10.1002/jrs.1250070606
35. Montagnac, Gilles (2019). SSHADE/REAP: Raman Experiments for Astrobiology and Planetology. SSHADE (OSUG Data Center). Service/Database. doi:10.26302/SSHADE/REAP
36. Thirumalai J (2017) Thin Film Processes: Artifacts on Surface Phenomena and Technological Facets, IntechOpen